NJC

New Journal of Chemistry

A journal for new directions in chemistry

Accepted Manuscript

This article can be cited before page numbers have been issued, to do this please use: Z. Chen, D. Li, L. Xu, Y. Jiang, K. Lin, Y. Zhao and J. Zhao, *New J. Chem.*, 2022, DOI: 10.1039/D2NJ01567F.

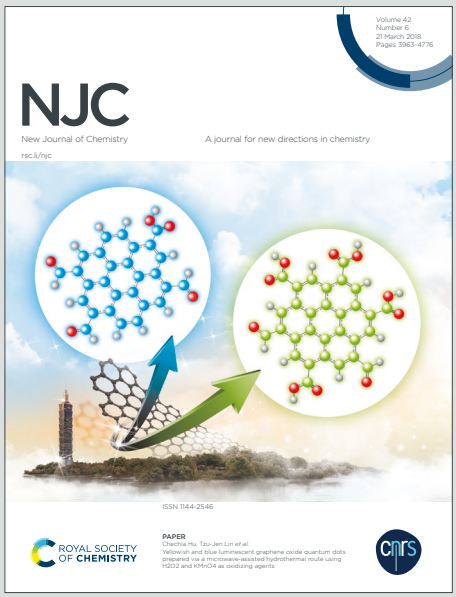

This is an Accepted Manuscript, which has been through the Royal Society of Chemistry peer review process and has been accepted for publication.

Accepted Manuscripts are published online shortly after acceptance, before technical editing, formatting and proof reading. Using this free service, authors can make their results available to the community, in citable form, before we publish the edited article. We will replace this Accepted Manuscript with the edited and formatted Advance Article as soon as it is available.

You can find more information about Accepted Manuscripts in the Information for Authors.

Please note that technical editing may introduce minor changes to the text and/or graphics, which may alter content. The journal's standard Terms & Conditions and the Ethical guidelines still apply. In no event shall the Royal Society of Chemistry be held responsible for any errors or omissions in this Accepted Manuscript or any consequences arising from the use of any information it contains.

Journal Name

ROYAL SOCIETY OF CHEMISTRY
View Article Online
DOI: 10.1039/D2NJ01567F

ARTICLE

Cationic metal-organic frameworks constructed from a trigonal imidazole-containing ligand for the removal of $Cr_2O_7^{2-}$ in water†

Received 00th January 20xx,
Accepted 00th January 20xx

DOI: 10.1039/x0xx00000x

www.rsc.org/

Zi-Peng Chen,[a] Ding Li,[a] Lei Xu,[b] Yu-Fei Jiang,[a] Kai Lin,*[c] Yue Zhao,*[a] and Jing Zhao*[a]

Recently, cationic metal-organic frameworks (MOFs) have drawn considerable attention in the treatment of wastewater containing toxic anions via anion exchange due to the presence of exchangeable anions in their pores. In this work, we employed a neutral imidazole-containing ligand tris(4-(1H-imidazol-1-yl)phenyl)amine (tipa) to construct two novel cationic MOFs, $\{[Ag_3(tipa)_2]_4\cdot[Ag(tipa)]\cdot(NO_3)_{13}\cdot 2CH_3CN\cdot 20H_2O\}$ (**1**) and $\{[Zn_{12}(H_2O)_{12}(tipa)_{12}(SiF_6)_9]\cdot(SiF_6)_2\cdot(OH)_2\cdot 7CH_3CN\cdot 64H_2O\}$ (**2**). Structural analysis revealed that complex **1** possessed 3D frameworks constructed from intercrossing 2D wave-like grids and highly disordered 1D chains with free NO_3^- in the channels, while **2** manifested 3D frameworks composed of rotaxane-like subunits with free SiF_6^{2-} and OH^- anions filled in the channels. Subsequently, these two MOFs were examined their anion exchange properties with $Cr_2O_7^{2-}$ and the results suggested that only compound **1** exhibited adsorption capacity for $Cr_2O_7^{2-}$ with high efficiency and recyclability.

Introduction

Water is the source of the lives and an indispensable substance in human life. However, with the population explosion and rapid development of industrial production, tens of thousands of pollutants have been extensively discharged into the water system and led to serious water pollution, which further aggravates the water source shortage and degrades ecosystems at the same time.[1-3] Currently, water safety problems have been recognized as one of the most urgent focuses that pose great threats to the sustainable development of human society and thus the development of efficient water decontamination methods has become one of the hot-spot issues in scientific research.[4] Among various water pollutants, those oxo-anionic contaminants containing heavy metal elements, such as $Cr_2O_7^{2-}$, CrO_4^-, MnO_4^-, ReO_4^-, TcO_4^- and so on, have attracted special attention because of their high toxicity and the difficulty of degradation.[5-10] As a well-known and common strong oxidant, $Cr_2O_7^{2-}$ has been widely used not only in the laboratory but also in various industrial fields, such as electroplating, paint, leather tanning, pesticides and so on and are massively poured into the environment along with industrial wastewater.[11-16] Furthermore, owing to the non-biodegradable nature and easy entry into human cells, $Cr_2O_7^{2-}$ anion could accumulate in living organisms and cause various diseases and damages, such as allergic reactions, ulcers, renal failure, and even some cancers, deformity, and gene mutation.[17-24] In the past decades, some methods and strategies have been developed to treat the toxic anion $Cr_2O_7^{2-}$ in wastewater and the absorption technique is recognized as one of the most promising candidates for $Cr_2O_7^{2-}$ removal due to the simple and convenient operation and high removal efficiency.[25] Therefore, it is of great significance to develop new absorbents to capture $Cr_2O_7^{2-}$ from water.

Metal-organic frameworks (MOFs) constructed from organic linkers and inorganic metal ions/clusters have emerged as a kind of the most fascinating crystalline porous organic-inorganic hybrid materials and aroused the intensive interest of researchers all around the world during the recent several decades.[26-30] Due to the large surface area, high porosity, easy modification and tunable structures, MOFs have shown attractive application prospects in different fields, such as gas adsorption/separation, energy storage, catalysis, optical materials, electronic devices, sensing, drug delivery and so on.[31-40] With the improvement of people's awareness of environmental protection, MOFs have also been explored extensively to remove pollutants and manifested as one of the most promising candidates for the removal of pollutants from aqueous and gaseous phases because of their superior performance.[3, 41] According to the charge of the coordination

[a] Coordination Chemistry Institute, State Key Laboratory of Coordination Chemistry, School of Chemistry and Chemical Engineering, Nanjing University, Nanjing 210023, China. E-mail address: jingzhao@nju.edu.cn (J. Zhao), zhaoyue@nju.edu.cn (Y. Zhao); Tel: +86 25 89681957

[b] Jiangsu Key Lab of Data Engineering and Knowledge Service, School of Information Management, Nanjing University, Nanjing 210023, China. E-mail address: xulei@nju.edu.cn (L. Xu)

[c] Jiangsu Environmental Resources Co., LTD, Nanjing 210019, China. E-mail address:368380386@qq.com (K. Lin)

†Electronic Supplementary Information (ESI) available: PXRD, EDS, fluorescence, UV-vis spectra and additional figures. CCDC 2160519 and 2064697. For ESI and crystallographic data in CIF or other electronic format see DOI:

View Article Online DOI: 10.1039/D2NJ01567E

networks, MOFs could be generally divided into three classes, namely anionic, neutral, and cationic MOFs. Compared to the other two MOFs, cationic MOFs are more likely to capture anionic pollutants from the water via ion-exchange process due to the potential strong electrostatic interactions between the electropositive skeleton and the trapped anionic species. Therefore, the synthesis of cationic MOFs and their application in the treatment of wastewater containing anionic pollutants have aroused special attention recently.[42-50] On the other hand, as one of the most widely used organic struts in the construction of MOFs, the neutral N-donor ligands have more access to afford cationic MOFs upon coordinated with cationic metal centers in comparison with another kind of most popular ligands, carboxylate ligands. For example, Li and coworkers utilized 4,4′-bis(1,2,4-triazole) (btr) and Ag(Ⅰ) to fabricate a novel cationic MOF with distorted octahedral and tetrahedral cages and applied it to the capture of $Cr_2O_7^{2-}$ via the ion-exchange process with ClO_4^-.[51] Desai et al. employed an imidazole-containing ligand, tris(4-(1H-imidazol-1-yl)phenyl)amine (tipa), to build a cationic Ni(Ⅱ)-based MOF containing free SO_4^{2-} in the channels that could be replaced by $Cr_2O_7^{2-}$ and MnO_4^- to realize the goal of removing toxic oxo-anions from water.[5] More impressively, the driving force and the capture mechanism in the above two reports could be elucidated by the single-crystal X-ray diffraction (SC-XRD) analysis.

Following the same strategy, we sought to adopt the neutral imidazole-containing ligand tipa to constitute cationic MOFs to remove toxic oxo-anions from water. By the reaction of tipa with $AgNO_3/ZnSiF_6$, we obtained two novel cationic MOFs, $\{[Ag_3(tipa)_2]_4\cdot[Ag(tipa)]\cdot(NO_3)_{13}\cdot 2CH_3CN\cdot 20H_2O\}$ (**1**) and $\{[Zn_{12}(H_2O)_{12}(tipa)_{12}(SiF_6)_9]\cdot(SiF_6)_2\cdot(OH)_2\cdot 7CH_3CN\cdot 64H_2O\}$ (**2**). SC-XRD analysis revealed that complex **1** exhibited a rare three-dimensional (3D) framework constructed from polycatenated wavelike grids and highly disordered one-dimensional (1D) chains and possessed 1D channels along a-axis, while complex **2** manifested a 3D framework constructed from self-interpenetrated rotaxane-like subunits with large cages. The inorganic anions NO_3^- in **1** and SiF_6^{2-}/OH^- in **2** functioned as the counterions filled in the channels or cages. Adsorption experiments indicated that complex **1** could capture $Cr_2O_7^{2-}$ with high efficiency and recyclability, while compound **2** hardly exhibited adsorption capacity for $Cr_2O_7^{2-}$.

Experimental

Materials and methods

All reagents and solvents were commercially purchased and used as received without further purification. Organic ligand tipa were synthesized according to the previously reported methods.[7] FT-IR spectra were recorded in the range of 400-4000 cm^{-1} on a Bruker Vector 22 FT-IR spectrophotometer using KBr pellets. Thermogravimetric analyses (TGA) were carried out on a NETZSCH STA 449F3 thermal analyzer under nitrogen with a heating rate of 10 °C min^{-1}. Powder X-ray diffraction (PXRD) data were collected at room temperature on bulk samples with Cu Kα radiation (1.54059 Å) on a Bruker D8 Advance X-ray diffractometer. UV-vis measurements were conducted at room temperature on a Shimadzu UV3600 spectrophotometer. Energy dispersive spectrometry (EDS) was measured on a field emission scanning electron micro-analyser (Hitachi S-4800).

Preparation of 1. Method Ⅰ: The saturated solution of tipa in CH_3CN (2 mL) was carefully layered on the solution of $AgNO_3$ (33.4 mg, 0.2 mmol) in deionized water (2mL). After standing for several days, nearly colorless block crystals of **1** could be obtained. Method Ⅱ: The mixture of $AgNO_3$ (33.4 mg, 0.2 mmol), tipa (11.1 mg, 0.025 mmol), CH_3CN (2.5 ml) and deionized water (2.5 mL) was sealed in a 10 mL plugged bottle and heated at 100 ℃ for 3 days. After cooling to room temperature, tiny colorless crystals could be obtained in 60 % yield based on the tipa ligand. IR (KBr pellet, cm^{-1}, Fig. S3†): 3440 (m, br), 3121 (m), 1655 (m), 1516 (s), 1383 (s), 1308 (w), 1282 (w), 1126 (w), 1065 (m), 963 (w), 829 (m), 726 (w), 652 (w), 546 (w).

Synthesis of 2. The preparation of **2** was almost same as that of **1** except that $ZnSiF_6\cdot 6H_2O$ (31.5 mg, 0.1 mmol) was used instead of $AgNO_3$ both in method Ⅰ and Ⅱ. Block crystals of **2** were obtained in 55% yield based on the tipa ligand with the method Ⅱ. IR (KBr pellet, cm^{-1}, Fig. S3†): 3431 (m, br), 3132 (m), 1626 (w), 1519 (vs), 1312 (m), 1290 (m), 1266 (m), 1126 (m), 1069 (s), 1019 (m), 967 (m), 834 (m), 735 (s), 654 (m), 541 (m), 475 (m).

Adsorption of $Cr_2O_7^{2-}$. The as-prepared samples of **1** and **2** (50 mg) were directly immersed in the aqueous solutions of $K_2Cr_2O_7$ (1 mM, 5.0 mL). The concentration of $Cr_2O_7^{2-}$ in the supernatant solution was monitored by the UV-vis measurements in the range of 250-800 nm. The absorbance intensities at 355 nm were used to calculate the adsorption efficiencies and the largest absorption amount.

X-ray crystallography

Single crystal X-ray diffraction (SC-XRD) data of **1** was collected on a Bruker D8 Venture Photon II diffractometer with graphite-monochromated Ga Kα radiation (λ = 1.34139 Å) using the φ–ω scan technique, while the SC-XRD data of **2** was collected on a Bruker D8 Venture Photon II diffractometer equipped with graphite-monochromated Mo Kα radiation Mo Kα radiation (λ = 0.71073 Å) using the φ–ω scan technique. The integration of diffraction data and intensity corrections for the Lorentz and polarization effects were performed by using SAINT program.[52] Semi-empirical absorption corrections were applied using SADABS program.[53] The structures were solved by direct methods with SHELXT-2018, expanded by subsequent Fourier-difference synthesis, and all the non-hydrogen atoms were refined anisotropically on F^2 using the full-matrix least-squares technique using the SHELXL-2019 crystallographic software package.[54, 55] The free solvent molecules in the unit cell have been taken into account to SQUEEZE option of the PLATON program.[53] Hydrogen atoms except those of coordinated water molecules were introduced at the calculated positions. The NO_3^- anions in **1** were quite highly disordered and a few parts of them can't even be determined so as to be taken into SQUEEZE option. Furthermore, the organic ligand tipa coordinated with Ag1 atoms in **1** was also highly disordered with two different orientations. All the carbon atoms on the benzene rings of tipa in **2** that were not bound to nitrogen atoms were disordered as well into two positions. The final chemical formulas were obtained based on volume/count electron analysis and TG analysis. The reported refinements were of the

View Article Online
DOI: 10.1039/D2NJ01567F

guest-free structures obtained by the SQUEEZE routine and the results were attached to the CIF files. Furthermore, due to the highly disordered nature of some nitrates and ligands in **1**, some restraints were used to make the structure reasonable and the refinement stable, which was also implied by the residual density map and fractal dimension plot (Fig. S1a†)[57]. The details of crystal parameters, data collection and refinements are listed in Table S1, and the selected bond lengths and angles are given in Table S2.

Results and discussion

Crystal structure description

Crystal structure of 1. According to the SC-XRD analysis, MOF **1** was crystallized in the orthorhombic system with space group of *Pnnn* and each asymmetric unit of **1** contained one quarter $\{[Ag_3(tipa)_2]_4\cdot[Ag(tipa)]\cdot(NO_3)_{13}\}$ molecule. As shown in Fig. S1b†, all the Ag(Ⅰ) atoms were coordinated with two nitrogen atoms from the adjacent tipa ligands. Further inspection into the structure of **1** revealed that the cationic frameworks consist of two parts: 3D $\{[Ag_3(tipa)_2]_4^{12+}\}_n$ coordination networks and 1D $\{[Ag(tipa)]^+\}_n$ coordination chains. In the 3D Ag-tipa networks, each imidazole ring of the ligands tipa bound to Ag(Ⅰ) cations to generate two-dimensional (2D) wavelike layers with numerous mesh openings (Fig. 1a and S1c†), which were large enough to allow the interpenetration of these 2D layers to form a 3D interlocking structure with 1D channels (Fig. 1b). Due to the high porosity, these cross-linked grids were also further interpenetrated with each other in a nearly orthogonal geometry to formulate the $\{[Ag_3(tipa)_2]_4^{12+}\}_n$ coordination networks with 1D channels along a-axis (Fig. 1c and Fig. S1d†). As for the 1D $\{[Ag(tipa)]^+\}_n$ coordination chains, the ligands tipa acted as a μ_2-bridging ligand with two of the imidazole rings of tipa connecting Ag(Ⅰ) cations to establish 1D $\{[Ag(tipa)]^+\}_n$ coordination chains (Fig. 1a). These chains were highly disordered to be filled in the channels of $\{[Ag_3(tipa)_2]_4^{12+}\}_n$ networks (Fig. 1d). Such complicated architecture constructed from four sets of wavelike coordination layers along with 1D chains running through the channels was hardly reported in previous studies. From the topological perspective, all the Ag^+ cations could be considered as 2-connected nodes, while the organic ligands tipa in the 3D networks and the 1D disordered chains could be treated as 3-connected and 2-connected linkers, respectively. Hence, the structure of **1** could be simplified as $\{12\cdot8\cdot12\}_2\{12^2\cdot14\}_2\{12^2\cdot8\}_2\{12\}_7\{8^3\}_2\{8\}_{10}$ symbol by using TOPOS software (Fig S1e†)[58]. In addition, a more in-depth analysis manifested that various noncovalent interactions, including the π…π, C-H…π, Ag(Ⅰ)…π, hydrogen bonding interactions and so on (Table S3†), played an important role in the formation of **1**. Although the porosity was distinctly reduced by self-interpenetration and stuffing, there were still quite considerable accessible channels remaining and enormous free NO_3^- anions were entrapped in these channels (Fig. S1f).

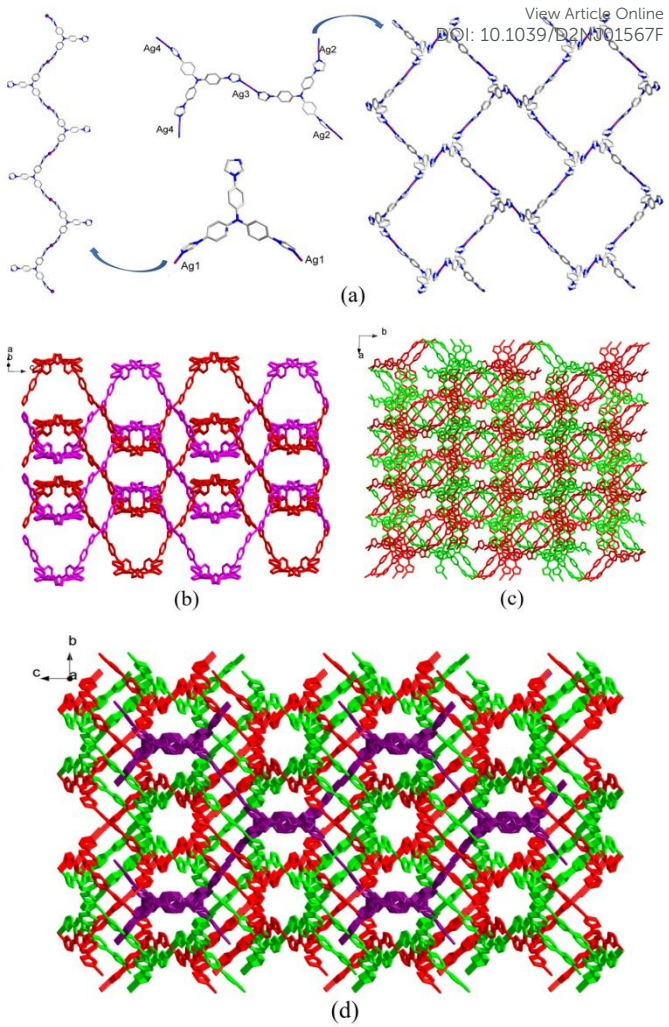

Fig. 1 (a) The coordination chains (left) or layers (right) based on the coordination between ligands tipa and Ag(Ⅰ) cations. (b) The 3D interlocking networks constructed from 2D wavelike reticulations. (c) The $\{[Ag_3(tipa)_2]_4^{12+}\}_n$ coordination networks along c-axis. (d) The final 3D cationic frameworks of **1**.

Crystal structure of 2. SC-XRD analysis revealed that complex **2** was crystallized in the trigonal *R*-3 space group and each asymmetric unit of **2** contained one quarter $\{[Zn_{12}(H_2O)_{12}(tipa)_{12}(SiF_6)_9]\cdot(SiF_6)_2\cdot(OH)_2\}$ molecule. As depicted in Fig. 2a, atoms Zn1 and Zn2 were both four-coordinated in a distorted trigonal pyramidal geometry (τ= 0.755 for Zn1; τ= 0.799 for Zn2)[59] surrounded by three nitrogen atoms from different tipa ligands (N5#1, N7, N8 for Zn1; N3#2, N12#3, N14) and one coordinated water molecule (O1 for Zn1; O2 for Zn2). Although all the Zn(Ⅱ) atoms connected three tipa ligands, the coordination between Zn1 and tipa formed one-dimensional (1D) trigonal windmill-like coordination chains (Fig. S2a†) while the binding of Zn2 with tipa generated pillared macrocyclic coordination rings (Fig. S2b†). More interestingly, the linkage of adjacent atoms Zn1, Zn2 and ligands tipa could form a cyclic coordination complex and the formed cyclic coordination complexes could interpenetrate with each other to fabricate a rotaxane-like substructure, whose components were further joined

View Article Online DOI: 10.1039/D2NJ01567F

together by neighboring tipa ligands (Fig. 2b). Through such complicated coordination bonds, 3D Zn-tipa coordination networks were built along with large pores and 1D channels along c-axis (Fig. S2c and S2d†). In the viewpoint of topology, the organic ligand tipa and Zn^{2+} cations could be both treated as 3-connected linkers and nodes, and thus structure of **2** could be simplified as a $\{3\cdot8^2\}\{3^2\cdot4\cdot8\cdot9^2\}\{3^3\cdot4\cdot6\cdot7^2\cdot8^2\cdot9\}\{3\}_2\{8\}$ symbol by using TOPOS software (Fig. S2e†). Apart from the strong coordination bonds, numerous noncovalent π…π and C-H…π interactions made great contributions to the formation of the final 3D Zn-tipa networks (Table S3†). The counter inorganic anions SiF_6^{2-} and OH^- were imprisoned in the channels and pores via various interactions, including the anion…π, hydrogen bonding, electrostatic interactions (SiF_6^{2-}…Zn^{2+}, F5…Zn1: 2.730 Å, F9…Zn2: 2.749 Å) and so on (Table S3†). The total solvent cavity volume of **2** was 27.3 % per unit cell calculated by PLATON.

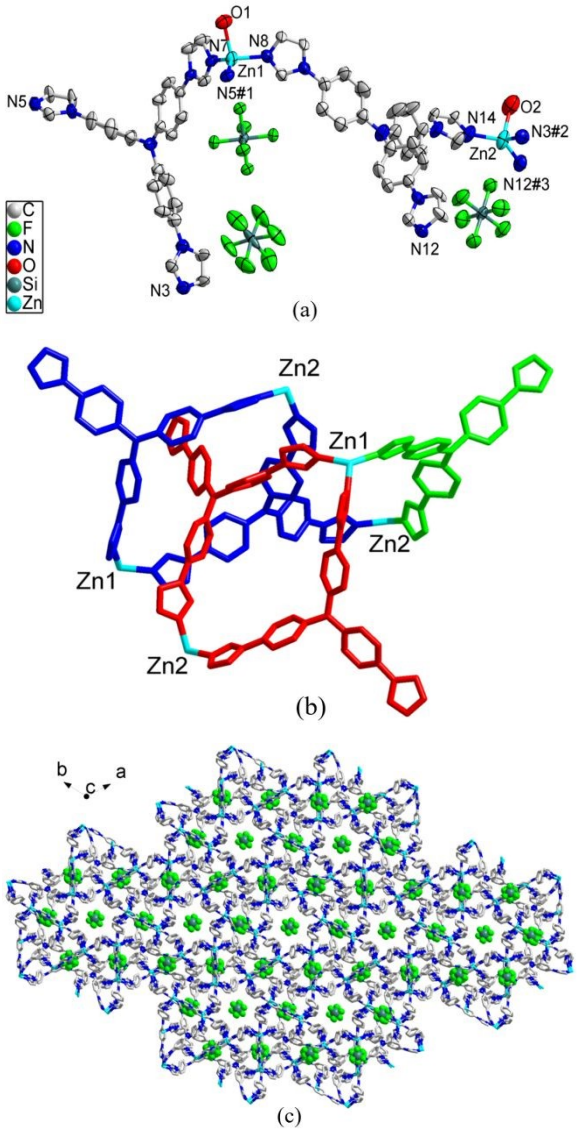

Fig. 2. (a) The coordination environment of Zn(II) in **2** with the ellipsoids drawn at the 30% probability level. The hydrogen atoms are omitted for clarity. Symmetric code: #1 y, -x+y+1, -z+1; #2 -x+y+1/3,-x+5/3,z-1/3; #3 x-y+2/3,x+1/3,-z+4/3 (b) The rotaxane-like substrcuture. (c) The final 3D coordiantion framewok of **2** with SiF_6^{2-} trapped in the pores.

PXRD and thermogravimetric stability

The bulk-phase purity and structural consistency of the as-synthesized MOFs were examined by the PXRD measurements. As shown in Fig. S4†, the experimental PXRD patterns of the prepared samples matched well with the simulated ones available from the crystallographic data, confirming that the as-synthesized samples of **1** and **2** were homogeneous and high phase-purity. In addition, the thermal stability of **1** and **2** were investigated by thermogravimetric (TG) measurements (Fig. S5†). Complex **1** showed a weight loss of 1.23% before 80 ºC and 5.85% between 80 and 180 ℃, corresponding to the release of 2 CH_3CN molecules (calcd 1.25%) and 20 water molecules (calcd 5.52%). Further weight loss was observed at 330 ºC owing to the decomposition of the framework. For complex **2**, the first weight loss of 2.62% was obtained before 75 ℃, corresponding to the release of 7 CH_3CN molecules (calcd 3.06 %). The second weight loss was 11.9 % between 75 and 160 ℃, which corresponded to the release of 64 water molecules (calcd 12.43 %) and the decomposition temperature was 290 ℃.

Capture of $Cr_2O_7^{2-}$ from aqueous solution

In consideration of the presence of free anions in the voids of **1** and **2**, we attempted to apply MOF **1** and **2** to the removal of the toxic oxo-anions, $Cr_2O_7^{2-}$. In order to examine whether the free anions (NO_3^- for **1**, SiF_6^{2-} and OH^- for **2**) were exchangeable with $Cr_2O_7^{2-}$, the crystalline samples of **1** and **2** (10 mg) are initially soaked in the aqueous solution of $Cr_2O_7^{2-}$ (10 mM, 10 mL). After standing at ambient conditions for several days, it can be found that the crystals of **1** turned from colorless to yellow completely, while the crystals of **2** remained almost colorless (Fig. 3a). Then, the excess crystal samples of **1** and **2** (50 mg) were immersed in the aqueous solutions of $Cr_2O_7^{2-}$ (2 mM, 5 mL), the color of the solution with samples of **1** become faded quickly and eventually nearly colorless while the solution that samples of **2** soaked in hardly changed (Fig. 3b). These phenomena indicated that MOF **1** could effectively remove $Cr_2O_7^{2-}$ from water while **2** barely exhibited adsorption capacity for $Cr_2O_7^{2-}$. Meanwhile, the resultant exchange solution of **1** was also monitored by the time-dependent UV-vis spectroscopy. As shown in Fig. 3c, it clearly showed that the intensity of the main characteristic adsorption peak of $Cr_2O_7^{2-}$ at 351 nm decreased quickly at the early stage and eventually reduced to quite close to zero within 20 h. According to the UV-vis spectra, the removal efficiency could be calculated using the formula $(I_0\text{-}I)/I_0$, where I_0 and I are the absorption peak intensities before and after soaking in the $Cr_2O_7^{2-}$ solution, respectively and it reached up to 94.5% within 20 h, indicating that the majority of toxic oxo-anion $Cr_2O_7^{2-}$ has been transferred from the solution into the crystals of **1**.

As we all know, capture selectivity and recyclability are important factors to evaluate the performance of absorbents. Hence, competitive adsorption experiments were carried out. 50 mg of the crystal samples of **1** were immersed in the mixed solution containing other anions (ClO_4^-, Cl^-, Br^-, SO_4^{2-}, and CO_3^{2-}) with the same concentration as $Cr_2O_7^{2-}$ (2 mM). After standing at room temperature

for 20 h, it can be found that the mixed solutions containing $Cr_2O_7^{2-}$ and interfering anions turned from yellow to nearly colorless (Fig. S6†). As illustrated in Fig. 4a, the removal efficiencies towards $Cr_2O_7^{2-}$ in the mixed solution was not reduced distinctly or even remained almost unchanged, showing that complex **1** could still catch $Cr_2O_7^{2-}$ in the presence of some other common anions and possess high selectivity and anti-interference for the capture of $Cr_2O_7^{2-}$. Furthermore, the recyclability of **1** for the capture of $Cr_2O_7^{2-}$ was checked as well in consideration of the practical applications. The sample of **1** after reaching the adsorption equilibrium in the $Cr_2O_7^{2-}$ solution was gathered by filtration and then soaked in the KNO_3 aqueous solution (100 mM). After standing at room temperature overnight, the supernatant solution turned from colorless to yellow and UV-vis measurement also showed the appearance of the characteristic absorption bands of $Cr_2O_7^{2-}$, which both demonstrated the release of $Cr_2O_7^{2-}$ (Fig. S7†). After repeated immersion in the fresh KNO_3 aqueous solution, the solid samples of **1** were separated by filtration and then applied to the EDS measurements. As shown in Fig. S8†, the peak corresponding to Cr at 5.42 eV was nearly negligible, suggesting that the desorption of $Cr_2O_7^{2-}$. Moreover, the treated samples of **1** were used to absorb $Cr_2O_7^{2-}$ again to check its reusability and the change in the color of the solution and UV-vis measurement both demonstrated the retainment of the capture capability towards $Cr_2O_7^{2-}$. After 5 cycles, the removal efficiency of **1** for $Cr_2O_7^{2-}$ was still up to 89.4 %, indicating the high recyclability of **1** (Fig. 4b).

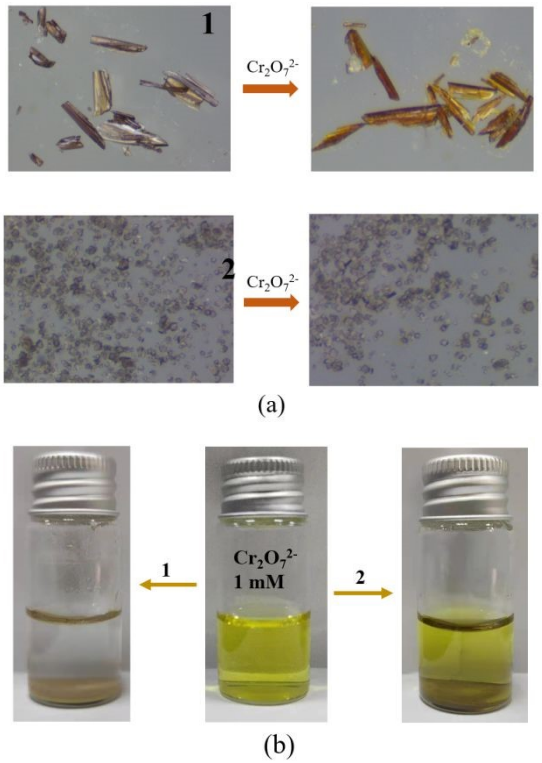

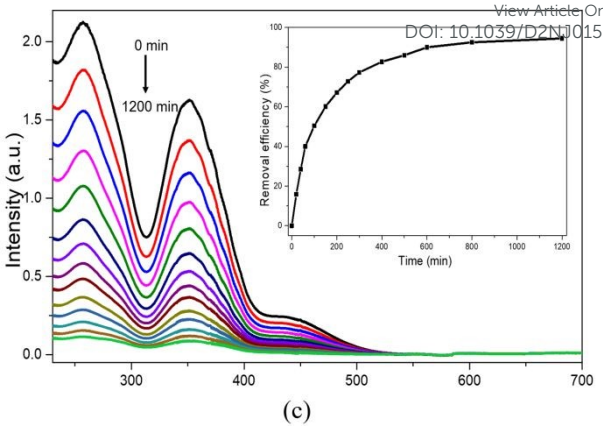

Fig. 3. (a) Optical microscopy images of the crystals of **1** and **2** before and after immersed in the aqueous solution of $Cr_2O_7^{2-}$ (10 mM). (b) The color changes of the $Cr_2O_7^{2-}$ solution after the addition of **1** and **2**. (c) Time-dependent UV-vis absorption spectra of $Cr_2O_7^{2-}$ solution upon the addition of **1** (inset: the absorbance of $Cr_2O_7^{2-}$ solution at 351 nm at a varied time).

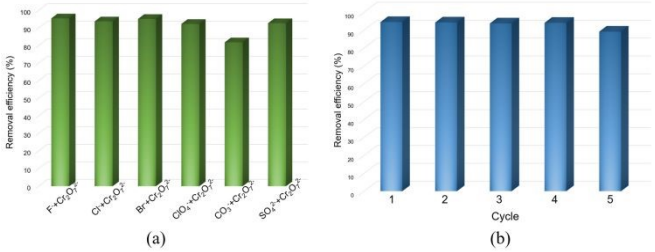

Fig. 4. (a) Effect of competing anions on the removal efficiency of $Cr_2O_7^{2-}$ by **1**. (b) The removal efficiency of **1** for $Cr_2O_7^{2-}$ in five cycles.

As a result of weak diffraction, SC-XRD studies could not be performed despite repeated attempts. Therefore, some other measurements including the PXRD, FT-IR and EDS were employed to demonstrate the anion exchange process between $Cr_2O_7^{2-}$ and NO_3^-. As shown in Fig. S9†, PXRD patterns of **1** after the adsorption of $Cr_2O_7^{2-}$ remained consistent with the as-synthesized samples, suggesting the retention of the crystallinity and the integrity of the framework of **1** during the adsorption process. The FT-IR spectrum in the solid samples **1** after soaking in the $Cr_2O_7^{2-}$ solution was almost identical with that of as-synthesized **1** except that the appearance of a new band corresponding to Cr-O stretching modes at 934 cm^{-1}, manifesting the adsorption of $Cr_2O_7^{2-}$ by **1** (Fig. S10†). In addition, EDS further confirmed the inclusion of $Cr_2O_7^{2-}$ into the channels of **1** because a new peak corresponding to the Cr element could be observed at 5.42 eV (Fig. S8†). A similar exchange process between NO_3^- and $Cr_2O_7^{2-}$ have been observed in some previous studies as well. On the other hand, the distances between Zn(II) cations and the F atoms of SiF_6^{2-} are so close to lead to the quite strong interactions between the anions and framework and the size of SiF_6^{2-} anions trapped in the pores are larger than the diameter of channels in **2** (Fig. S11†), hence it is difficult for **2** to capture $Cr_2O_7^{2-}$ by the exchange with SiF_6^{2-}. According to the crystal structure, the openings/windows of the pores in **1** and **2** were both estimated to be about 5 Å (Fig. S12). As for the anions, on the one hand, the size of SiF_6^{2-} are larger than NO_3^-; on the other hand, SiF_6^{2-} is an octahedral

anion while NO_3^- is a planar anion. Therefore, it is much more difficult for SiF_6^{2-} to be released from the pores than NO_3^-.

Conclusions

In this work, we employed a neutral imidazole-containing ligand tipa to react with $AgNO_3/ZnSiF_6$ to fabricate two novel cationic MOFs with 3D frameworks. Structural analysis revealed that the cationic framework of **1** was constituted by the integration of the highly disordered 1D coordination Ag-tipa chains and the interpenetrated networks of 2D tipa-Ag layers, while compound **2** manifested 3D cationic framework constructed from self-interpenetrated rotaxane-like Zn-tipa coordination networks with large cages. The inorganic anions NO_3^- in **1** and SiF_6^{2-}/OH^- in **2** functioned as the counter anions to occupy the voids of the coordination networks. Absorption experiments demonstrated that compound **1** could remove $Cr_2O_7^{2-}$ from water effectively with high selectivity and recyclability, while compound **2** hardly exhibited capture capability for $Cr_2O_7^{2-}$. This work indicated the important role of the size of free anions for cationic MOFs to capture toxic anions and would contribute positively to the design and synthesis of MOF-based sorbents.

Acknowledgements

We acknowledge the National Natural Science Foundation of China (grant nos. 21401099, 21671099 and 91753121) and the Shenzhen Basic Research Program (JCYJ20180508182240106).

Notes and references

1 C. Tortajada, P. V. Rensburg, *Nature*, 2020, **577**, 26-28.
2 *The United Nations World Water Development Report 2017.*, United Nations Educational, Scientific and Cultural Organization, Paris, 2017.
3 J. Li, H. Wang, X. Yuan, J. Zhang, J. W. Chew, *Coord. Chem. Rev.*, 2020, **404**, 213116.
4 R. M. Rego, G. Kuriya, M. D. Kurkuri, M. Kigga, *J. Hazard. Mater.*, 2021, **403**, 123605.
5 A. V. Desai, B. Manna, A. Karmakar, A. Sahu, S. K. Ghosh, *Angew. Chem. Int. Ed.*, 2016, **55**, 7811-7815.
6 M. Chen, W.-M. Xu, J.-Y. Tian, H. Cui, J.-X. Zhang, C.-S. Liu, M. Du, *J. Mater. Chem. C*, 2017, **5**, 2015-2021.
7 H. R. Fu, Y. Zhao, Z. Zhou, X. G. Yang, L. F. Ma, *Dalton Trans.*, 2018, **47**, 3725-3732.
8 S. Rapti, D. Sarma, S. A. Diamantis, E. Skliri, G. S. Armatas, A. C. Tsipis, Y. S. Hassan, M. Alkordi, C. D. Malliakas, M. G. Kanatzidis, T. Lazarides, J. C. Plakatouras, M. J. Manos, *J. Mater. Chem. A*, 2017, **5**, 14707-14719.
9 Y. Wang, M. S. Xie, J. H. Lan, L. Y. Yuan, J. P. Yu, J. Q. Li, J. Peng, Zh. F. Chai, J. K. Gibson, M. L. Zhai, W. Q. Shi, *Chem*, 2020, **6**, 2796-2809.
10 L. N. Pincus, H. E. Rudel, P. V. Petrovic, S. Gupta, P. Westerhoff, C. L. Muhich, J. B. Zimmerman, *Environ. Sci. Technol.*, 2020, **54**, 9769-9790.
11 B. Dhal, H. N. Thatoi, N. N. Das, B. D. Pandey, *J. Hazard. Mater.*, 2013, **250-251**, 272-291.
12 M. Elavarasi, A. Rajeshwari, S. A. Alex, D. N. Kumar, N. Chandrasekaran, A. Mukherjee, *Anal. Methods*, 2014, **6**, 5161-5167.
13 H. R. Fu, N. Wang, J. H. Qin, M. L. Han, L. F. Ma, F. Wang, *Chem. Commun.*, 2018, **54**, 11645-11648.
14 S. Kumar, E. Alveroğlu, A. Balouch, F. N. Talpur, M. S. Jagirani, Abdullah, A. M. Mahar, A. H. Pato, D. Mal, S. Lal, *New J. Chem.*, 2020, **44**, 18668-18678.
15 Y. Su, Y. Wang, X. Li, X. Li, R. Wang, *ACS Appl. Mater. Interfaces*, 2016, **8**, 18904-18911.
16 W. Liu, Y. Wang, Z. Bai, Y. Li, Y. Wang, L. Chen, L. Xu, J. Diwu, Z. Chai, S. Wang, *ACS Appl. Mater. Interfaces*, 2017, **9**, 16448-16457.
17 J. Liu, Y. Ye, X. Sun, B. Liu, G. Li, Z. Liang, Y. Liu, *J. Mater. Chem. A*, 2019, **7**, 16833-16841.
18 Y. Abshirini, H. Esmaeili, R. Foroutan, *Mater. Res. Express*, 2019, **6**, 125513.
19 W. A. El-Mehalmey, A. H. Ibrahim, A. A. Abugable, M. H. Hassan, R. R. Haikal, S. G. Karakalos, O. Zaki, M. H. Alkordi, *J. Mater. Chem. A*, 2018, **6**, 2742-2751.
20 H. R. Fu, Z. X. Xu, J. Zhang, *Chem. Mater.*, 2014, **27**, 205-210.
21 Y. H. Zou, J. Liang, C. He, Y. B. Huang, R. Cao, *Dalton Trans.*, 2019, **48**, 6680-6684.
22 G. P. Li, G. Liu, Y. Z. Li, L. Hou, Y. Y. Wang, Z. Zhu, *Inorg. Chem.*, 2016, **55**, 3952-3959.
23 P. Rekha, R. Muhammad, V. Sharma, M. Ramteke, P. Mohanty, *J. Mater. Chem. A*, 2016, **4**, 17866-17874.
24 P. Samanta, P. Chandra, S. Dutta, A. V. Desai, S. K. Ghosh, *Chem. Sci.*, 2018, **9**, 7874-7881.
25 Y. Zhao, L. Li, B. Ding, X. G. Wang, Z. Y. Liu, E. C. Yang, X. J. Zhao, *Dalton Trans.*, 2020, DOI: 10.1039/d0dt03662e.
26 N. W. Ockwig, O. Delgado-Friedrichs, M. O'Keeffe, O. M. Yaghi, *Acc. Chem. Res.*, 2005, **38**, 176-182.
27 S. Natarajan, P. Mahata, *Chem. Soc. Rev.*, 2009, **38**, 2304-2318.
28 O. K. Farha, J. T. Hupp, *Acc. Chem. Res.*, 2010, **43**, 1166-1175.
29 S. Yuan, L. Feng, K. Wang, J. Pang, M. Bosch, C. Lollar, Y. Sun, J. Qin, X. Yang, P. Zhang, Q. Wang, L. Zou, Y. Zhang, L. Zhang, Y. Fang, J. Li, H. C. Zhou, *Adv. Mater.*, 2018, **30**, e1704303.
30 N. Stock, S. Biswas, *Chem. Rev.*, 2012, **112**, 933-969.
31 J. R. Li, R. J. Kuppler, H. C. Zhou, *Chem. Soc. Rev.*, 2009, **38**, 1477-1504.
32 M. D. Allendorf, C. A. Bauer, R. K. Bhakta, R. J. T. Houk, *Chem. Soc. Rev.*, 2009, **38**, 1330-1352.
33 J. Lee, O. K. Farha, J. Roberts, K. A. Scheidt, S. T. Nguyen, J. T. Hupp, *Chem. Soc. Rev.*, 2009, **38**, 1450-1459.
34 Z. Hu, B. J. Deibert, J. Li, *Chem. Soc. Rev.*, 2014, **43**, 5815-5840.
35 V. Stavila, A. A. Talin, M. D. Allendorf, *Chem. Soc. Rev.*, 2014, **43**, 5994-6010.
36 W. Xia, A. Mahmood, R. Zou, Q. Xu, *Energy Environ. Sci.*, 2015, **8**, 1837-1866.
37 L. Sun, M. G. Campbell, M. Dinca, *Angew. Chem. Int. Ed.*, 2016, **55**, 3566-3579.
38 L. Wang, Y. Han, X. Feng, J. Zhou, P. Qi, B. Wang, *Coord. Chem. Rev.*, 2016, **307**, 361-381.
39 R. Medishetty, J. K. Zareba, D. Mayer, M. Samoc, R. A. Fischer, *Chem. Soc. Rev.*, 2017, **46**, 4976-5004.
40 M. X. Wu, Y. W. Yang, *Adv. Mater.*, 2017, **29**, 1606134.
41 N. A. Khan, Z. Hasan, S. H. Jhung, *J. Hazard. Mater.*, 2013, **244-245**, 444-456.

View Article Online
DOI: 10.1039/D2NJ01567F

42 A. V. Desai, A. Roy, P. Samanta, B. Manna, S. K. Ghosh, *iScience*, 2018, **3**, 21-30.
43 J. Yuan, L. Xiao, G. Y. Huang, J. M. Yang, H. B. Zhu, *ChemNanoMat*, 2020, **6**, 1776-1781.
44 S. Sharma, A. V. Desai, B. Joarder, S. K. Ghosh, *Angew. Chem. Int. Ed.*, 2020, **132**, 7862-7866.
45 D. P. Sheng, L. Zhu, X. Dai, C. Xu, P. Li, C. I. Pearce, C. L. Xiao, J. Chen, R. H. Zhou, T. Duan, O. K. Farha, Z. F. Chai, S. Wang, *Angew. Chem. Int. Ed.*, 2019, **58**, 4968-4972.
46 S. Dutta, P. Samanta, B. Joarder, S. Let, D. Mahato, R. Babarao, S. K. Ghosh, *ACS Appl. Mater. Interfaces*, 2020, **12**, 41810-41818.
47 C. Jiang, R. P. Sun, Z. Y. Du, V. Singh, S. Chen, *New J. Chem.*, 2020, **44**, 12646-12653.
48 N. N. Yang, L. J. Zhou, P. Li, Q. Sui, E. Q.g Gao, *Chem. Sci.*, 2019,**10**, 3307-3314.
49 M. Y. Guo, P. Li, S. L. Yang, R. Bu, X. Q. Piao, E. Q. Gao, *ACS Appl. Mater. Interfaces*, 2020, **12**, 43958-43966.
50 G. Li, W. S. Liu, S. L. Yang, L. Zhang, R. Bu, E. Q. Gao, *Inorg. Chem.*, 2022, **61**, 902-910.
51 X. Li, H. Xu, F. Kong, R. Wang, *Angew. Chem. Int. Ed.*, 2013, **52**, 13769-13773.
52 SAINT*, Program for Data Extraction and Reduction*, Bruker AXS, Inc., Madison, WI, 2001.
53 G. M. Sheldrick, *SADABS*, *Program for Empirical Adsorption Correction of Area Detector Data*. University of Gottingen, Gottingen, Germany, 2003.
54 G. M. Sheldrick, *SHELXS-2018, Program for the Crystal Structure Solution*, University of Gottingen, Gottingen, Germany, 2018.
55 G. M. Sheldrick, *SHELXL-2018, Program for the Crystal Structure Solution*, University of Gottingen, Gottingen, Germany, 2018.
56 (a) A. L. Spek, *Acta Crystallogr., Sect. A: Fundam. Crystallogr.*, 1990, **46**, 194; (b) A. L. Spek, PLATON, *A Multipurpose Crystallographic Tool*, Utrecht University, Utrecht, The Netherlands, 2005, or Spek, A. L. *J. Appl. Cryst*. 2003, **36**, 7.
57 K. Meindl, J. Henn, *Acta Cryst.*, 2008, **A64**, 404-418.
58 V. A. Blatov, *TOPOS*, A Multipurpose Crystallochemical Analysis with the Program Package, Samara State University, Russia, 2009.
59 L. Yang, D. R. Powell, R. P. Houser, *Dalton Trans.*, 2007, 955-964.